Journal of
Nanoscience and Nanotechnology
Vol. 12, 1–7, 2012

Vertically Aligned Carbon Nanotubes for Microelectrode Arrays Applications

J. R. Castro Smirnov[1], Eric Jover[1], Roger Amade[1], Gemma Gabriel[2], Rosa Villa[2], and Enric Bertran[1,*]

[1] *FEMAN Group, Department of Applied Physics and Optics, IN2UB, Universitat De Barcelona, C/ Martí i Franquès, 1, 08028, Barcelona, Spain*
[2] *Instituto De Microelectrónica De Barcelona (IMB-CNM-CSIC), Campus UAB, 08193 Bellaterra, Spain*

In this work a methodology to fabricate carbon nanotube based electrodes using plasma enhanced chemical vapour deposition has been explored and defined. The final integrated microelectrode based devices should present specific properties that make them suitable for microelectrode arrays applications. The methodology studied has been focused on the preparation of highly regular and dense vertically aligned carbon nanotube (VACNT) mat compatible with the standard lithography used for microelectrode arrays technology.

Keywords: Nanostructured Materials, Carbon Nanotubes (CNTs), Vertically Aligned Carbon Nanotubes (VACNTs), Plasma Enhanced Chemical Vapour Deposition (PECVD), Micro-Electrode Arrays (MEAS).

RESEARCH ARTICLE

1. INTRODUCTION

Since the introduction of carbon nanotubes (CNTs) by Smalley,[1] and the first experiments done by Ijima in 1991,[2] this new form of nanomaterial transformed deeply the research world wide. Taking into account their attractive mechanical, thermal, electrical and physical properties in general, CNTs can compete and even overmatch the best metals or semiconductors in the market. Because of this, CNTs have gathered large variety of applications[3] and has made them ideal for their use in electronics and, in particular, as biocatalytical electrodes,[4] interconnexion of biosystems to solid state electronic devices[5] and micro-electrode arrays (MEAS).[6,7] Micro-electrode arrays (MEAs) (Fig. 1) have been established as a well-known technique for interfacing with neural assemblies.[8,9] In addition, they are now recognized as one of the main approaches for the design of neural prosthetic devices to artificially restore impaired neural function (e.g., for vision, hearing and limb movement).[10] Vertically aligned carbon nanotubes (VACNTs) have suitable characteristics[11–15] for micro and nano electronics because they are highly regular and compact and have an adequate morphology as electrodes. Moreover, density and structure of carbon nanotubes are important characteristics in electrochemical applications because they affect the electrochemical behavior of the electrode. Also, the layout of VACNTs, with a high density and connected one by one to the metal electrode increases the efficiency of contact and is useful in the area of biosensors, where availability of sites for both biomolecule binding and electron transfer is needed.

In general, micro-electrode arrays are based on a proton conductive membrane attached between anode and cathode. The two electrodes have an active catalyst layer that makes possible the electrochemical reaction and a diffusion support that grants mechanical stability and improved electrical contact.[14,16] Compared to macro-electrodes, it offers numerous advantages due to the miniaturization of the system. This opens the door to several applications.[17–22]

For example, the ability to perform electrochemical analysis at reduced scale allows the study of electrolyte volume bellow one micro-litre, so that experiments on biological samples *in vivo* can be done without having destructive character, given the low current involved. CNT coatings offer a novel and stimulating direction to further improve the performances of MEAs[23] as a result of their many useful properties such as mechanical stability, chemical durability, high electrical conductance[24] and their biocompatibility.[25] CNT coated electrodes show evidence of remarkably high specific surface, appropriate for this kind of applications. Furthermore, it was recently demonstrated that CNT based electrodes improve neuronal electrical signaling.[26] In particular, multi-walled carbon nanotubes

*Author to whom correspondence should be addressed.

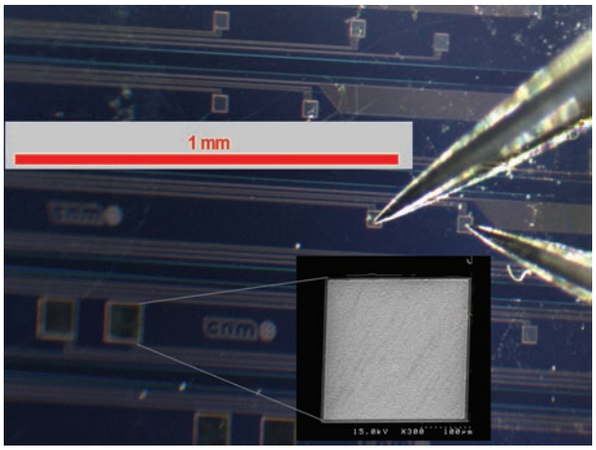

Fig. 1. General view of a MEA. SEM view of CNTs deposited on one of the square electrodes (inserted image).

(MWCNTs)[27] have a suitable surface structure to withstand subsequent treatment with plasma, such as discussed below.

In spite of the advantages offered by VACNTs for MEAs applications, there are very few studies proposing them for neural networks monitoring.[28] Although MEAs have become useful research implements, they are distant from being optimized for durable implantation. While several results have been found for MEAS preparation through CVD, Plasma-enhanced CVD represents a better-quality and reachable method for CNT growth, requiring a high vacuum and temperature system, along with the assistance provided by an electric field allowing vertical alignment of CNTs. Furthermore, VACNTs have advantages regarding voltammetric measurements over CVD-grown ones. These results demonstrate the huge potential of such nanostructured materials to make possible an interface between the neural system and state of the art nano-electronics. It is the purpose of this work to obtain experimental evidence of the superior properties gained with VACNT grown over recently made and designed MEAS.

In this paper, we have optimized the fabrication process of VACNTs on MEAs for electrically analyzing alive neural tissues, in order to improve the introduction of nutrients during the monitoring time.

2. EXPERIMENTAL DETAILS

The production of CNTs was performed in a PECVD reactor, made by the FEMAN group. It consists on three homemade magnetron sputtering heads, which permit the deposition of layers of different catalysts and other materials depending on the target installed (Fe, Ni, Co, Si) plus a complete PECVD system.

All parameters and measures were operated by from a LabView (National Instruments) program. In order to reach desired temperatures, a Xantrex heater power supply (XDC 60-100) was used. Working in a high vacuum is important to avoid oxidation of the sample and to ensure effectiveness in the sputtering and PECVD processes. With that purpose, we used three different pumps, for different levels of vacuum. From atmospheric pressure to $\sim 2 \cdot 10^3$ Pa, a rotatory pump (EV25 QS AL, Leybold Vacuum GmbH) was enabled. From $\sim 2 \cdot 10^3$ to $\sim 3 \cdot 10^{-2}$ Pa a roots pump (WU 251, Leybold-Heraus RUVAC, Germany) and from $\sim 3 \cdot 10^{-2}$ to $\sim 4 \cdot 10^{-4}$ Pa a turbomolecular pump was used (Turbovac 361C, Leybold Vacuum GmbH, Germany).

2.1. Growing CNTs Over MEAS

The CNTs growing process onto microelectrode arrays was more complicated than the procedure onto a standard silicon wafer. The process is described in three step diagrams showing the internal structure of a MEAS (Fig. 2). First, MEAs devices were coated by a patterned PMMA

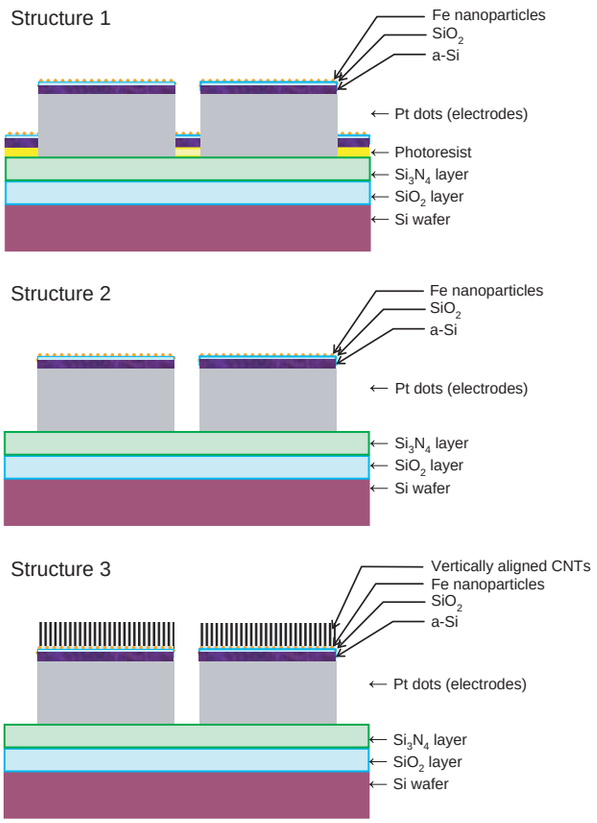

Fig. 2. Schematic representation of the steps carried out to growth VACNTs on the structure of MEAs devices. *Structure 1*: Schematic of a MEAs device with a patterned PMMA layer covering the interspaces between the Pt electrodes and having: (a) an a-Si thin layer (~20 nm), (b) a diffusion barrier layer of SiO_2/a-Si, formed by oxidation at air, and (c) a Fe ultrathin layer deposited at RT by sputtering performing a nucleation layer for CNTs growth. *Structure 2*: Schematic of the electrode after the lift-off process. *Structure 3*: Schematic of the electrode after deposition of CNTs by PECVD.

RESEARCH ARTICLE

layer covering the interspaces between the Pt electrodes. Starting from this structure, an a-Si thin layer (∼20 nm thick) was deposited on the samples at room temperature (RT) by magnetron sputtering from a c-Si target. Then, samples were taken out of the reactor and exposed to air for 15 minutes to form a thin surface layer of SiO_x. Finally, a Fe ultrathin layer was deposited by magnetron sputtering at RT on the SiO_x (structure 1, Fig. 2). SiO_x acts as a diffusion barrier by minimizing the diffusion of Fe atoms toward the substrate and to maintain the ability of Fe catalyst.[29] In order to study the effect of the Fe nanoparticle size on the growth of CNTs, Fe layers were deposited in the range of 3 to 10 nm.

To ensure that the CNTs only grow over the electrodes, a lift-off process was conducted afterwards (structure 2, Fig. 2). The lift-off process was used to patterning the microelectrode using a sacrificial material, in this case a photo-resist. Isopropanol and acetone were used as solvents and the sample was sonicated during 30 s upon Fe and Si layers remained only in the regions having a direct contact with the platinum electrodes. When the process was finished, the samples were dried with nitrogen and reintroduced inside the reactor. Later, an annealing treatment was done before the last step consisting in the VACNTs growth by PECVD, assisted by hot filament (structure 3, Fig. 2). By this method, VACNTs only grow on the electrodes coated by Fe nanoparticles.

TEM images corresponding to CNTs grown on metallic electrodes using PECVD can be seen in Figure 3, where Fe nanoparticles appear isolated on the tip of CNTs and play the role of catalyzing the growth of CNT structures. In order to remove amorphous carbon and Fe catalyst particles from the tip of the CNTs, a slight water plasma treatment was performed after the PECVD growing process. This last treatment increases the specific area and electron transfer capability.[14, 30]

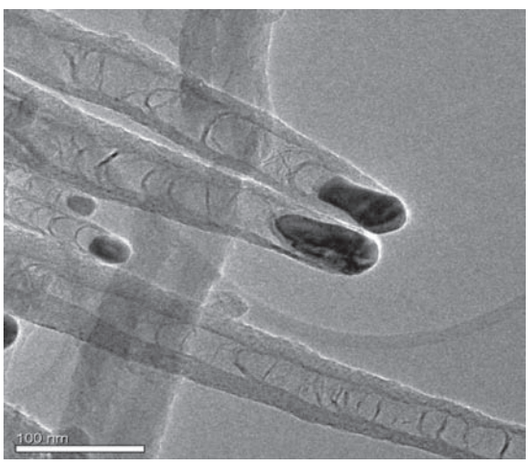

Fig. 3. TEM images showing the catalyst nanoparticles on the tip of the CNTs.

3. RESULTS AND DISCUSSION

The first attempt to grow CNTs over MEAs was based on the optimal parameters obtained in a previous work done by the FEMAN group.[31] After deposition of the Fe layer, a process of lift-off was performed to remove the PMMA and to open the areas outside the Pt electrodes.

Next step was the nanostructuration of the Fe layer in order to produce nanoparticles. As a general rule, films with few nanometers produce smaller particles and short nanotube diameters. At the same time, because the sputtered films at RT had not an isolated grain structure, an annealing was necessary to fracture the film in nanoparticles (structure 2 of Fig. 4). Samples were annealed at 800 °C in a reductive atmosphere ($Ar + H_2$) and few minutes were enough to form small Fe nanoparticles on the electrodes. Usually, this operation facilitates the coalescence of Fe nucleous deposited on the SiO_2/a-Si diffusion barrier and, the resulting Fe particles have a size that depends of the Fe layer thickness. This size, in turn, limits the diameter of the CNTs. Another important detail concerns to the surface state of the Fe nanoparticles. Thus, in order to clean the surface of the Fe nanoparticles before the growth of carbon nanotubes, we applied argon plasma before entering the carbon precursor gas.

The annealing process lasted 800 s. During this period, a ramp temperature of 10 °C/s was used to reach the set point (680 °C). The temperature was stabilized after 60 or 120 s. Additional 30 s were necessary for purging hydrogen by the insertion of NH_3. Then, the carbon precursor was entered in the chamber and CNTs were grown during 900 s.

Figure 4(a) shows one of the preliminary results of growth of vertically aligned carbon nanotubes (VACNTs) on Pt electrodes. The irregular density observed in Figure 4(a) points to an unequal diffusion process with domain sizes of 10 to 20 μm. In these earlier experiments, the diffusion of Fe into the Pt electrodes was higher than directly into silicon wafers and, only some isolated and short CNTs were obtained on Pt electrodes. Hence, the a-Si layer thickness was increased to avoid Fe diffusion. Moreover, in order to optimize the CNTs growing process, the Fe layer thickness was explored in the range of 3 to 10 nm. The results plotted in Figure 4(c) point to a maximum growth rate of CNTs for a Fe layer of 5 nm. This can be explained by the confluence of two mechanisms, diffusion and nucleation. First, the diffusion of Fe atoms toward the substrate is limited by the thickness of the silicon layer and, second, the onset of nucleation of CNTs occurs when C concentration in Fe nanoparticles reaches a critical value, which depends on the limit of solubility of carbon in iron. Samples with larger Fe nanoparticles (for 7 and 10 nm Fe layers) show shorter CNTs probably due to a delay in the beginning of nucleation and to the formation of an amorphous carbon layer on Fe nanoparticles.

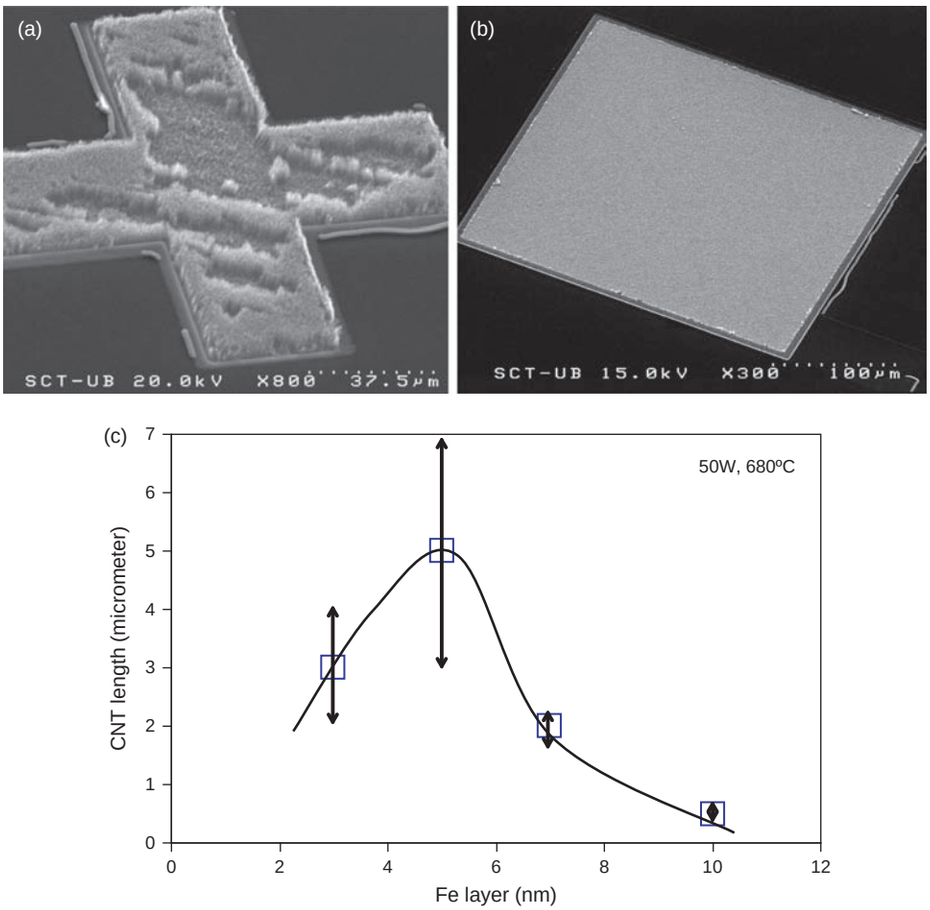

Fig. 4. (a) SEM image of MEAS where diffusion phenomena can be seen. (b) SEM image of MEAs with 20 and 10 nm layer thickness for Si and Fe respectively. (c) CNT length as a function of the thickness of the Fe catalyst layer. The maximum of growth rate corresponds to 5 nm of Fe layer.

RESEARCH ARTICLE

For MEAs applications and in order to optimize the electrochemical characteristics of CNTs, a CNTs length of 0.5–3 μm was chosen. Figure 4(b) shows an example of a homogeneous growth of CNTs on the structure Fe/SiO_x/a-Si/Pt formed by an a-Si layer of 20 nm and a Fe layer of 10 nm.

Figure 5(a) shows an example of the resulting CNTs with a length of 500 nm, which form a dense and homogeneous mat. This surface morphology results from a highly selective growth of CNTs, only on Pt electrodes, which avoids possible electrical short-circuits between wires, pads and electrodes.

Other PECVD parameters, such as temperature, reaction time, and plasma power were also explored to determine their effects on the CNTs growth. Figure 5(c) shows the increase of CNT length as RF power increases. The PECVD process parameters for this experiment were 640 °C of substrate temperature, 50 W of RF power, 20 nm of a-Si layer and 5 nm of Fe layer. The increase of temperature did not affect the length of the CNTs significantly in the explored range. However, although it is not evident from the SEM images exposed here, an accurate study showed that the average diameter of the CNTs increases with the growth temperature. In addition, a decrease in temperature down to 650 °C, together with a Fe layer of 5 nm, resulted in an increase in the CNTs length from 0.5 μm to about 2 μm, while maintaining the uniformity across the electrode (Fig. 5(b)).

The diameter of nanotubes also depends on the Fe nanoparticles size. Usually, each nanoparticle of Fe leads to the creation of one CNT, and the density of carbon nanotube is limited by the density of Fe nanoparticles resulting from the annealing process.

The growing process described in this work has resulted in multi-wall CNTs with a "bamboo-like" structure with a diameter in the range of 40 to 60 nm (Fig. 3).

An important parameter of the kinetics of growth is the activation energy, E_{act}. PECVD is a film growth technique based on plasma, in which the excited species react with each other in the gas phase. This makes it possible to deposit films at lower substrate temperatures than with thermal CVD, in which a high substrate temperature is necessary to cross over the activation energy. The Arrhenius plot of ln (growth rate) versus $1/T$ (K) was used to

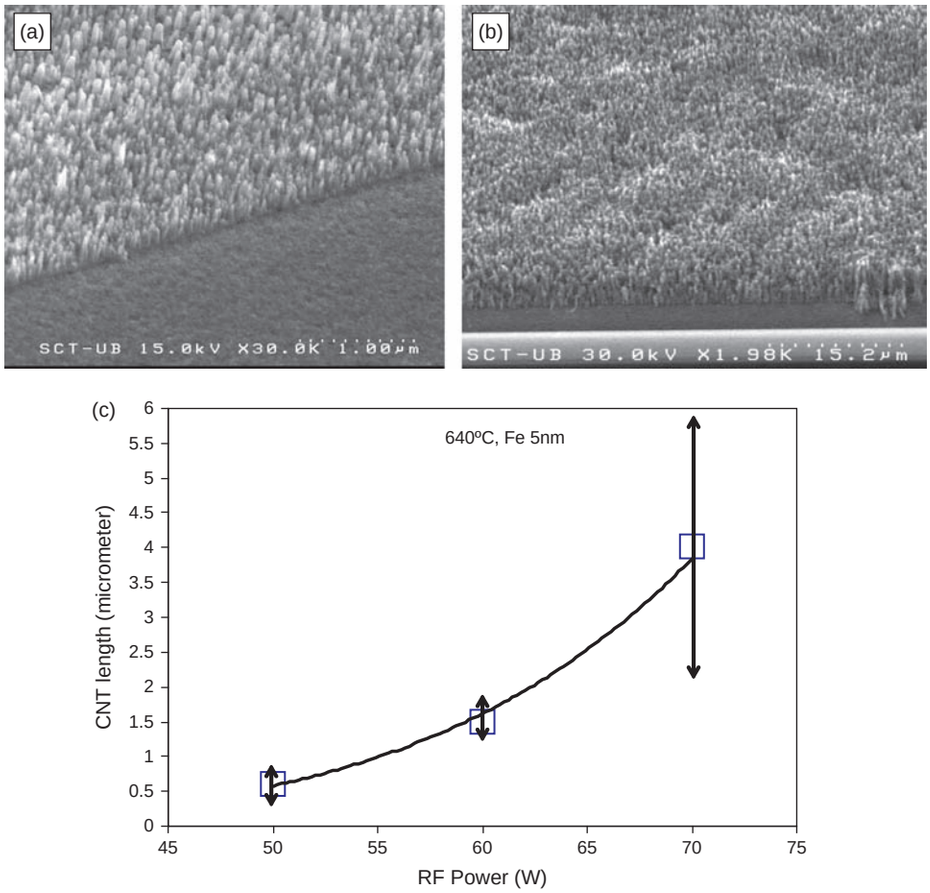

Fig. 5. (a) Micrography of 500 nm CNTs grown onto a MEAs Pt electrode. (b) Longer CNTs were obtained at 650 °C keeping the homogeneity. (c) CNT length as a function of the RF power during the PECVD process. Samples were grown at 5 nm of the Fe catalyst layer thickness and 640 °C of substrat temperature.

derive E_{act}. The growth rate can be dependent on the size of catalytic particles.

According to the temperature dependence of the growth rate R of CNTs:

$$R = R_0 e^{-E_{act}/kT}$$

where R_0 is the growth rate at 0 K. A series of VACNTs samples grown at temperatures between 640–700 °C and 60 ± 10 W of RF power was used to obtain E_{act}. The Arrhenius plot of Figure 6 provides an activation energy E_{act} value of the CNT growth of around 28 kcal/mol (1.2 eV). This value agrees reasonably well with that of a growing process activated by temperature rather than by plasma (0.23 eV).[34, 35] In our case, the process needed plasma treatment during the CNTs growth to produce VACNTs. The obtained lower growth rates compared to the results of Ducati et al.[35] (factor close to 2) are probably due to differences in the growing parameters and the intensity of ion bombardment during our PECVD process.

Raman spectroscopy measurements provided the quality of the CNTs (Fig. 7(a)). The left peak corresponds to the D band, which is related to the content of amorphous

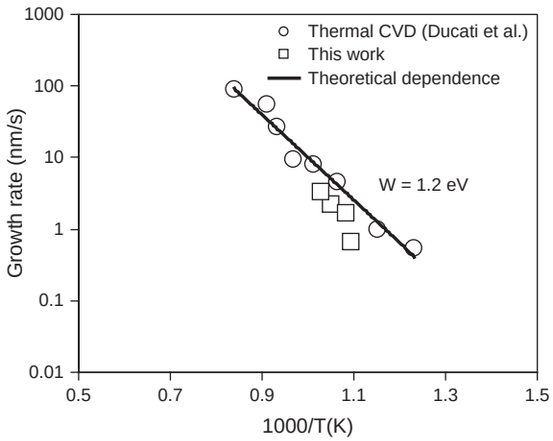

Fig. 6. The growth rate variation with temperature for thermal CVD and PECVD. The plotted squares correspond to VACNTs samples grown at 60 ± 10 W of RF power, on Fe(5 nm)/Si(20 nm)/Pt structures. The data points for thermal CVD are from Ref. [35].

RESEARCH ARTICLE

carbon and the existence of defects. The G band (right peak) is related to the presence of graphitic carbon. The D–G ratio points to the purity of the CNTs. Thus, after performing a water plasma treatment of CNTs, an increase in the G band was detected (Fig. 7(a)), which accounts for an increase of CNTs purity. According to previous reported results, water plasma oxidizes amorphous carbon producing CO_2.[14] The CNTs presented in this work were systematically exposed to a water plasma at low RF power during 5 min in order to purify and to maintain their original strength.

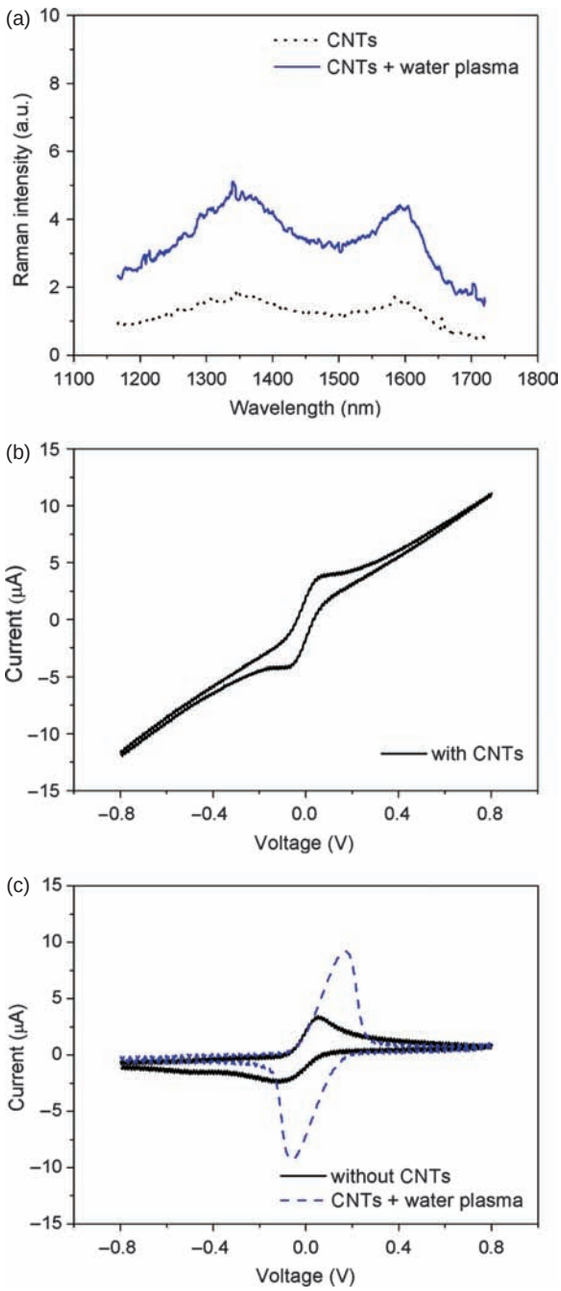

Fig. 7. (a) Raman intensity versus wavelength before and after water plasma treatment. (b) Cyclic voltammetry analysis of the MEAS with CNTs and no water plasma. (c) Comparation of cyclic voltammetry characteristics of MEAS devices having bare electrodes and water plasma treated CNTs deposited by PECVD on electrodes.

The electrochemical characteristics of the CNTs deposited on the MEAs samples were determined by cyclic voltammetry. The used solution consisted of 5 mM $Fe(CN)_6^{4-}$ in 0.2 M Na_2SO_4. An Au electrode was used as pseudo-reference electrode. The working and counter electrodes consisted of W tips connected to the MEAs pads, as shown in Figure 1. Figure 7(b) shows a cyclic voltammogram of a CNT based MEAs sample without water plasma treatment. Clearly, the presence of amorphous carbon results in a low intensity signal and high capacitive currents. Figure 7(c) shows a comparison between the results of cyclic voltammetry of a MEAs sample without CNTs and a sample with water plasma-treated CNTs. The peak current of the sample with water plasma-treated CNTs is near three times more intense than for the sample without CNTs. Moreover, the position of the peak has shifted to higher potentials pointing to a faster ion diffusion and to an increase of the electronic transfer as a consequence of the water plasma treatment.[14] Cyclic voltammetry and pulsed voltammetry are common techniques to characterize the electrochemical properties of CNT arrays.[32, 33] The values obtained are close to other results obtained in literature and suitable for MEAs applications.

4. CONCLUSIONS

CNTs grown by PECVD between 640 °C and 680 °C from Fe catalyst layer between 5 and 10 nm have an adequate morphology and structure for MEAs applications. Vertically aligned, uniform and highly dense CNTs were obtained after a complementary process combining magnetron sputtering, annealing (defining the size and density of Fe nanoislands) and PECVD. Structure and morphology determined by electron microscopy (SEM and TEM) have shown a high quality electrode delimited areas previously defined by lithography. The electrodes appear uniformly covered by a dense CNTs mat with a thickness of few microns. Concerning these results, we remark the growth of a diffusion barrier of Si (minimum of 20 nm) and Fe (10 nm) layer, that are needed to ensure homogeneity over the electrodes at relatively high temperature (around 680 °C). The VACNTs growth activation energy was determined to be 1.2 eV, which corresponds to a thermally activated CVD growth. Cyclic voltammetry measurements demonstrated that the quality of the CNTs improved after a water plasma treatment. CNTs for biomedical applications (1.5 μm length) can be produced by the described PECVD assisted by hot filament technology. The improved electrochemical properties of the VACNTs electrodes, their easy and simple micro-fabrication procedure, as well as their bio-compatibility and durability, suggest that VACNTs electrodes have an enormous

potential for micro and nanoelectronics applications in biomedicine, micro electrode arrays (MEAs) (Fig. 1) for the connection of neuronal assemblies.

Acknowledgments: One of the authors J. R. Castro Smirnov thanks to the MAE of Spanish Government for funding the 2009–2010 grant. This work was supported by AGAUR of Generalitat de Catalunya (project 2009GR00185) and by MICINN of Spanish Government (project CTQ2009-14674-C02-01). Authors acknowledge SCT-UB for their technical support in SEM and TEM images.

References and Notes

1. T. Guo, C. Jin, and R. E. Smalley, *J. Phys. Chem.* 95, 4948 (**1991**).
2. S. IJima, *Nature* 354, 56 (**1991**).
3. R. H. Baughman, A. A. Zakhidov, and W. A. de Heer, *Science* 297, 787 (**2002**).
4. D. Wang, J. J. Rack, and L. Chen, *J. Nanosci. Nanotechnol.* 9, 2310 (**2009**).
5. A. M. Cassell, J. Li, T.-D. B. Nguyen-Vu, J. E. Koehne, H. Chen, R. Andrews, and M. Meyyappan, *J. Nanosci. Nanotechnol.* 9, 5038 (**2009**).
6. K. Wang, H. A. Fishman, H. Dai, and J. S. Harris, *Nano Lett.* 6, 2043 (**2006**).
7. E. Ben-Jacob and Y. Hanein, *J. Mater. Chem.* 18, 5181 (**2006**).
8. G. Buzsáki, *Nat. Neurosci.* 7, 446 (**2004**).
9. D. Eytan and S. Marom, *J. Neurosci.* 26, 8465 (**2006**).
10. S. Berber, Y. K. Kwon, and D. Tomanek, *Phys. Rev. Lett.* 84, 4613 (**2000**).
11. W. C. Hu, L. M. Yuan, Z. Chen, D. W. Gong, and K. Saito, *J. Nanosci. Nanotechnol.* 2, 203 (**2002**).
12. W. B. Choi, E. Bae, D. Kang, S. Chae, B. Cheong, J. Ko, E. Lee, and W. Park, *Nanotechnology* 15, 512 (**2004**).
13. E. Einarsson, M. Kadowaki, K. Ogura, J. Okawa, R. Xiang, Z. Zhang, T. Yamamoto, Y. Ikuhara, and S. Maruyama, *J. Nanosci. Nanotechnol.* 8, 6093 (**2008**).
14. F. J. Del Campo, J. García-Céspedes, F. X. Muñoz, and E. Bertran, *Electrochem. Commun.* 10, 1242 (**2008**).
15. G. Cabral, E. Titus, D. S. Misra, and J. Gracio, *J. Nanosci. Nanotechnol.* 8, 4029 (**2008**).
16. T. V. Reshetenko, H.-T. Kim, and H.-J. Kweon, *Electrochimica Acta* 53, 3043 (**2008**).
17. R. M. Wightman and D. O. Wipf, *Electroanal. Chem.* 15, 267 (**1989**).
18. A. M. Bond, *Analyst* 11, 119 (**1994**).
19. R. J. Forster, *Chem. Soc. Rev.* 23, 289 (**1994**).
20. C. G. Zoski, *Electroanalysis* 14, 1041 (**2002**).
21. R. Feeney and S. P. Kounaves, *Electroanalysis* 12, 677 (**2000**).
22. C. A. Thomas, P. A. Springer, G. E. Loeb, Y. Berwald-Netter, and L. M. Okun, *Exp. Cell Res.* 74, 61 (**1972**).
23. E. W. Keefer, B. R. Botterman, M. I. Romero, A. F. Rossi, and G. W. Gross, *Nature Nanotechnol.* 3, 434 (**2008**).
24. D. Danailov and P. Keblinski, *J. Nanosci. Nanotechnol.* 2, 503 (**2002**).
25. S. Garibaldi, C. Brunelli, and V. Bavastrello, *Nanotechnology* 17, 391 (**2006**).
26. V. Lovat, D. Pantarotto, L. Lagostena, B. Cacciari, M. Grandolfo, M. Righi, G. Spalluto, M. Prato, and L. Ballerini, *Nano Lett.* 5, 1107 (**2005**).
27. H. Kim, K.-Y. Chun, J. Choi, Y. Kim, and S. Baik, *J. Nanosci. Nanotechnol.* 10, 3362 (**2010**).
28. K. A. Seger, E. de Asis, W. K. Wong, L. Wong, J. J. Hieb, C. Yang, and M. S. Isaacson, Digest of the LEOS Summer Topical Meetings, 69 (**2008**).
29. C. Liu, A.-J. Cheng, M. Clark, and Y. Tzeng, *Diamond Relat. Mater.* 14, 835 (**2005**).
30. T. Gabay, M. Ben-David, I. Kalifa, and R. Sorkin, *Nanotechnology* 18, 035201 (**2007**).
31. R. Amade, E. Jover, B. Caglar, T. Mutlu, and E. Bertran, *J. Power Sources* 196, 5779 (**2011**).
32. J. Kohenne, J. Li, A. M. Cassell, H. Chen, Q. Ye, H. Tee Ng, J. Han, and M. Meyyappan, *J. Mater. Chem.* 14, 676 (**2004**).
33. A. O. Fung, C. Tsiokos, O. Paydar, L. H. Chen, S. Jin, Y. Wang, and J. W. Judy, *Nano Lett.* 10, 4321 (**2010**).
34. S. Hofmann, B. Kleinsorge, C. Ducati, and J. Robertson, *New J. Phys.* 5, 153.1 (**2003**).
35. C. Ducati, I. Alexandrou, M. Chhowalla, G. A. J. Amaratunga, and J. Robertson, *J. Appl. Phys.* 92, 3299 (**2002**).

Received: 29 November 2011. Accepted: 17 January 2012.

RESEARCH ARTICLE